

# Three-dimensional Mapping with Augmented Navigation Cost through Deep Learning

Felipe G. Oliveira<sup>\*1,2</sup>, Mario F. M. Campos<sup>1</sup>, and Douglas G. Macharet<sup>1</sup>

<sup>1</sup> Computer Vision and Robotics Lab. (VeRLab), Dep. of Computer Science, Universidade Federal de Minas Gerais (UFMG). Belo Horizonte 31270-901, Brazil.

{felipegomes, mario, doug}@dcc.ufmg.br.

<sup>2</sup> Institute of Exact Sciences and Technology (ICET), Universidade Federal do Amazonas (UFAM). Itacoatiara 69103-340, Brazil.

felipeoliveira@ufam.edu.br

**Abstract.** This work addresses the problem of mapping terrain features based on inertial and LiDAR measurements to estimate the navigation cost for an autonomous ground robot. Unlike most indoor applications, where surfaces are usually human-made, flat, and structured, external environments may be unpredictable regarding the types and conditions of the travel surfaces, such as traction characteristics and inclination. Attaining full autonomy in outdoor environments requires a mobile ground robot to perform the fundamental localization and mapping tasks in unfamiliar environments, but with the added challenge of unknown terrain conditions. A fuller representation of the environment is fundamental to increase confidence and to reduce navigation costs. To this end, we propose a methodology composed of five main steps: *i*) speed-invariant inertial transformation; *ii*) roughness level classification; *iii*) navigation cost estimation; *iv*) sensor fusion through Deep Learning; and *v*) estimation of navigation costs for untraveled regions. To validate the methodology, we carried out experiments using ground robots in different outdoor environments with different terrain characteristics. Results show that the terrain maps thus obtained are a faithful representation of outdoor environments allowing for accurate and reliable path planning.

PhD Thesis to be considered in CTDR. Conclusion: 26/08/2020. Full text, associated publications, and videos of the results are available at: <http://www.dcc.ufmg.br/~felipegomes/doutorado>.

## 1 Introduction

Autonomous navigation for ground robots in unstructured outdoor environments has been the focus of numerous research efforts in Field Robotics in the past few years [6]. Challenges range from localization and mapping to navigation with obstacle avoidance of both static and dynamic objects. External natural environments are especially challenging for ground robots as they exhibit heterogeneous roughness surfaces, including vegetation, pebbles, sand, mud, snow, ice patches, and water puddles. Such surfaces may also be irregular and present different slopes, which significantly increase the difficulty for ground robots to perform

their tasks successfully [5]. A promising route towards solving this challenge is to augment the robot’s maps with rich, informative data streams, which would allow the robot to estimate the *navigation cost* (difficulty) of traversing different areas more accurately.

Typical approaches used to obtain Navigation Cost Maps such as [9] map an outdoor environment with estimates of navigation costs for various robot poses. However, most of the works in state-of-the-art literature focus on the response of a single sensor, which potentially constrains the ability to generate accurate navigation costs [6, 5, 4].

In this work, we propose a learning-based multi-sensor approach for generating an outdoor terrain cost map, based on the fusion of inertial measurements and LiDAR data. Our approach provides the potential to improve the autonomous navigation of ground robots in an external unstructured environment, as illustrated in Fig. 1. By combining information provided by different sensory modalities, we can assign navigation costs across a global map. The generated cost maps are combined with traditional path planning approaches to generate optimal paths across the map, optimizing aspects such as traveled distance, time, or energy expenditure.

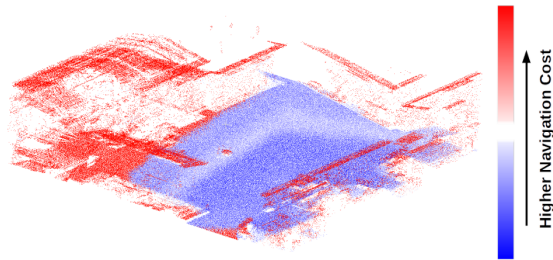


Fig. 1: Three-dimensional outdoor map with associated terrain navigation cost. This is an excerpt of a larger result presented in the experiments section.

### 1.1 Contributions

This work’s main contribution is the multimodal representation of unknown terrain. The representation mentioned above is based on the prediction of inertial measurements from LiDAR data regarding speed-invariant inertial signals. Our methodology trains a Convolutional Neural Network (CNN) on recorded LiDAR and IMU data, and learns to predict navigation costs for previously-unseen terrain patches. Additionally, we have contributions in:

- **Inertial speed-invariant transformation:** We propose an inertial data transformation method to reduce the impact of speed variation during inertial data acquisition, resulting in a speed-invariant terrain signature;
- **Roughness level classification:** A roughness level classification is presented to associate an irregularity level to a travelled patch on unknown and unstructured terrains, from inertial data defined in frequency domain;
- **Navigation cost representation:** A high level terrain representation is proposed to combine the main features in outdoor environments, such as

roughness and slope, through a regression model, defining the level of difficulty to navigate on a region;

- **Outdoor terrain mapping:** We propose a 3D navigation cost mapping approach to represent outdoor environments, regarding inertial data and geometric data, presenting a reliable and effective terrain representation to improve the autonomous navigation of ground robots.

The contributions of this work are published in the main conferences in the area [8][7]. Furthermore, some contributions are under review on an international journal.

## 2 Methodology

This section presents our multi-sensor terrain mapping method, whose overview is illustrated in Fig. 2. For better understanding, we divided our approach into the following three main stages, which will be further detailed in the next subsections: *i*) Three-dimensional mapping and localization; *ii*) Navigation cost estimation using inertial data; and *iii*) Map augmentation through deep learning.

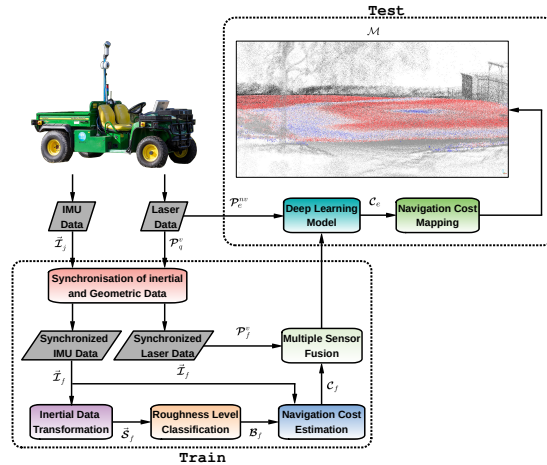


Fig. 2: Overview of the proposed outdoor terrain mapping, composed of the steps: *i*) Synchronisation of inertial and geometric data; *ii*) Speed-Invariant Transformation; *iii*) Roughness Level Classification; *iv*) Navigation Cost Estimation; *v*) Multiple Sensor Fusion; and *vi*) Navigation Cost Mapping.

### 2.1 Three-Dimensional Mapping and Localization

The technique we use to create the three-dimensional map is called C-SLAM, firstly presented in [1]. A more recent version using a 3D Velodyne PUCK LiDAR instead of the 2D Hokuyo LiDAR was presented in [11]. The C-SLAM builds accurate 3D maps from a sequence of point cloud measurements, acquired during the robot motion. A 6Degrees of Freedom (DOF) Inertial Measurement Unit (IMU) sensor is used to align the point clouds with the trajectory, and a

3D spinning LiDAR sensor, mounted on the ground vehicle, acquires the point clouds. Additionally, from C-SLAM, a precise approach is proposed to estimate the robot localization, combined with wheel odometry, called C-LOC (please refer to [11] for further details).

## 2.2 Navigation Cost Estimation using Inertial Data

Inertial data provides an effective and straightforward way to quantify the difficulty to traverse an unknown and unstructured outdoor environment [6]. However, inertial data are highly affected by variation in the robot’s velocity profile. Therefore, before dealing with roughness and slope estimations, it is necessary to address the speed variation issue. Then, the roughness level classification is performed, and finally, the cost function will combine the mentioned features into a single measurement, which is called navigation cost.

**Inertial speed-invariant transformation** The proper use of inertial information to represent terrain irregularities should take speed into account. For a given surface, lower speeds lead to lower inertial magnitudes, while higher speeds lead to higher magnitudes [8]. To mitigate this problem, we propose to use the Inertial Speed-Invariant Transformation (ISIT) function.

We propose two ISIT, regarding the inertial data: *i*) linear acceleration along the Z-axis; and *ii*) angular velocity along the Y-axis. Both functions share the same model, presented in equation 1. However, the first function addresses the transformation of the linear acceleration in Z-axis, while the second function addresses the transformation of angular velocity in Y-axis. The equation:

$$\vec{\mathcal{S}}_f = \varphi\left(\vec{\mathcal{I}}_f, \nu_c, \nu_g\right) = \vec{\mathcal{I}}_f \times \eta(\nu_c, \nu_g), \quad (1)$$

defines a function that receives as input the inertial data  $\vec{\mathcal{I}}_f$ , the current robot’s speed  $\nu_c$  and the goal speed  $\nu_g$ . Additionally, the function learns a transformation factor  $\eta(\nu_c, \nu_g)$ , that maps  $\vec{\mathcal{I}}_f$ , acquired at different speeds, into inertial measurements at constant speed  $\vec{\mathcal{S}}_f$ . To estimate the transformation factor, a multiple quadratic regression ( $\eta(\nu_c, \nu_g)$ ) is applied, which is defined as:

$$y^s = b_0^s + b_1^s \cdot x_1^s + b_2^s \cdot x_2^s + b_3^s \cdot x_1^{s2} + b_4^s \cdot x_2^{s2} + b_5^s \cdot x_1^s \cdot x_2^s + \varepsilon, \quad (2)$$

where  $y^s$  are the predicted transformation factors,  $x^s$  are the components of model matrix, and  $b^s$  are the regression parameters to speed-invariant transformation problem.  $\varepsilon$  is the regression model error.

**Roughness level classification** One of the most important features to represent an outdoor environment is the terrain roughness, commonly obtained from inertial sensors. In this work, an IMU is used to acquire linear accelerations and angular velocities.

In order to process the data from the inertial sensor, we apply a Fast Fourier Transform (FFT) to convert the raw speed-invariant inertial data ( $\vec{\mathcal{S}}_f$ ), from time domain to frequency domain depicting 1024 frequencies [12]. For every

inertial data (linear acceleration along the Z-axis and angular velocity about the Y-axis), we observe that not all 1024 frequencies are discriminant enough for a good roughness representation [2]. Based on several samples, we noticed that considering the first 300 frequencies for every inertial data would suffice. With individual features for linear acceleration along Z-axis and angular velocity about Y-axis, both representations are concatenated, resulting in a roughness descriptor.

From the roughness descriptors and the respective known roughness levels, we trained a supervised classification model. With the classification model ( $\mathcal{C}$ ), it is possible to classify the roughness levels ( $\mathcal{B}_f$ ), given speed-invariant inertial data ( $\vec{\mathcal{S}}_f$ ), during the robot motion. The  $\mathcal{B}_f$  value is rescaled to the range [0...1], where 1 is the maximum roughness level.

**Navigation cost estimation** In this work, we propose a navigation cost function  $\psi(\cdot)$ , which considers three input data: *i*) roughness level ( $\mathcal{B}_f$ ); *ii*) roll orientation ( $\vec{\mathcal{I}}_f$ ); and *iii*) pitch orientation ( $\vec{\mathcal{P}}_f$ ) [7]. The roughness level is defined in the previous Subsection. Roll and pitch orientations inform how inclined the robot is, in  $X$  and  $Y$  axes. Both roughness and slope of the terrain can make moving impractical on outdoor terrain. In this work, we consider the level of roughness and the level of attitude equally weighted.

To achieve the expected navigation cost, estimated by  $\psi(\cdot)$ , we first apply an attitude function ( $\vartheta(\cdot)$ ) that combines roll and pitch orientations, to obtain an overall representation of the terrain slope. The attitude cost, estimated by  $\vartheta(\cdot)$ , is scaled within the range [0...1], with 1 being the maximum attitude cost. The attitude cost and roughness level are applied to the navigation cost function  $\psi(\cdot)$ , providing a high-level representation of navigability. The navigation cost ( $\mathcal{C}_f$ ), estimated by  $\psi(\cdot)$ , is scaled to [0...1] range, where 1 is the maximum cost.

Functions  $\vartheta(\cdot)$  and  $\psi(\cdot)$  are based on application of a 3rd degree polynomial regression, chosen because it is the lowest polynomial degree that sufficiently fits the predefined Lookup Table (LUT) with the expected values. The 3rd degree polynomial regression model presents the following structure:

$$y^c = b_0^c + b_1^c.x_1^c + b_2^c.x_2^c + b_3^c.x_1^c.x_2^c + b_4^c.x_1^{c2} + b_5^c.x_2^{c2} + b_6^c.x_1^{c2}.x_2^c + b_7^c.x_1^c.x_2^{c2} + b_8^c.x_1^{c3} + b_9^c.x_2^{c3}, \quad (3)$$

where  $y^c$  are the predicted transformation factors,  $x^c$  are the components of model matrix, and  $b^c$  are the regression parameters to the navigation cost estimation problem.  $\varepsilon$  is the regression model error.

### 2.3 Map Augmentation through Deep Learning

Here we address the creation of a learning-augmented navigation cost map for an outdoor environment. Our predictive model learns the relation between navigation costs, computed from inertial data, and point clouds, extracted from geometric data. A global continuous three-dimensional map is created to represent the navigation costs, corresponding to the level of difficulty to navigate throughout a terrain.

**Synchronisation of Inertial and Geometric Data** We propose an approach to synchronize data provided by different types of sensors. The IMU collects inertial data ( $i_j$ ) from the robot’s current location, whereas the laser collects geometric data ( $p_q^v$ ) from regions visited by the robot, regarding the known three-dimensional map. Then, to compute the navigation cost for a position  $(x, y)$ , it is necessary to find the inertial and geometric measurements that correspond to the same respective coordinate ( $g_f^v$ ).

From each visited coordinate ( $g_f^v$ ), we extract a point cloud ( $p_f^v$ ) that corresponds to a visited region ( $r_f^v$ ). The region’s area is related to the robot’s dimensions, which corresponds to an approximation of the real Gator’s length and width, i.e., 3.0 m x 2.0 m.

From the point cloud ( $p_f^v$ ) that is contained in the region ( $r_f^v$ ), it is necessary to identify the inertial data ( $i_f$ ) that corresponds to the same region. By overlaying the trajectory with the map, considering the measurement timestamps, we can spatially reference the two measurements and assign them to the visited region ( $r_f^v$ ).

**Multisensor Fusion** In order to achieve a more complete representation of the surrounding terrain, it is necessary to estimate the inertial navigation costs ( $\mathcal{C}_e$ ) for unvisited (unknown) coordinates. This process takes into account laser measurements ( $\mathcal{P}_e^u$ ) around the robot as prior knowledge for the navigation cost predictor.

Our proposed predictive model is based on a class of deep learning architectures called CNN [13]. The proposed CNN predictive model will learn the relationship between inertial and LiDAR measurements, combining data provided by different sensors. A CNN receives as input a two-dimensional matrix, which is computed from a point cloud ( $\mathcal{P}_f^v$  or  $\mathcal{P}_e^u$ ), i.e., a set of three-dimensional and continuous points, contained in a region ( $r_f^v$  or  $r_e^u$ ). To convert the three-dimensional points into a two-dimensional grid, the region is discretized regarding a 0.05 resolution, resulting in 60x40 cells. The average of the points is computed for each cell, regarding Z-axis (height), obtaining a two-dimensional terrain grid.

The proposed CNN architecture is composed of: *i*) Convolutional layer; *ii*) Rectified linear unit (ReLU); *iii*) Batch normalization; *iv*) Pooling; *v*) Dropout; *vi*) Fully-connected layer; and *vii*) Fully-connected linear activation layer. For the proposed approach, four convolutional units composed by Convolutional, Batch normalization, ReLU, and Max-pool layers, are applied.

**Navigation Cost Mapping** This problem is related to the assignment of estimated navigation cost ( $\mathcal{C}_e$ ) to the respective three-dimensional coordinate in the Navigation Cost Map ( $\mathcal{M}$ ). The estimated navigation cost ( $\mathcal{C}_e$ ) is computed from a point cloud ( $\mathcal{P}_e^u$ ). This point cloud ( $\mathcal{P}_e^u$ ) is extracted from an unvisited coordinate ( $g_e^u$ ) and is contained in a region ( $r_e^u$ ), centered in the referred coordinate ( $g_e^u$ ). The estimated navigation cost ( $\mathcal{C}_e$ ) is then assigned to the respective coordinate ( $g_e^u$ ) in the Navigation Cost Map ( $\mathcal{M}$ ).

To select the unvisited coordinate, we first take into account the set of visited coordinates ( $\mathcal{G}^v$ ), and for each visited coordinate ( $g_f^v$ ) we define a neighborhood.

We then predict navigation cost for every unvisited coordinate within this neighborhood range. This process is repeatedly performed for unvisited points. We finally obtain a 3D Augmented Terrain Map, comprised of 3D points and their respective navigation costs.

### 3 Experiments

#### 3.1 Experimental setup

Experiments were conducted using: *i*) a 49.7 cm x 50.8 cm *Pioneer P3-AT* equipped with an IMU *Xsens MTi*, a GPS, and a laptop (Fig. 3a). The different velocities applied to the robots were set to 0.4, 0.6 and 0.8 m/s and the robots were tele-operated with a joystick; and *ii*) a 1.3 m x 2.7 m *John Deere Gator*, equipped with an IMU *MicroStrain 3DM-CV5-25*, a *Velodyne VLP-16* and an on-board computer (Fig. 3b). The robot was driven manually, so its velocity was not regulated. The coordinate system for both robots considers: *i*) X-axis points towards the robot front; *ii*) Y-axis points to the left side of the robot; and *iii*) Z-axis is obtained accordingly to the right-hand rule.

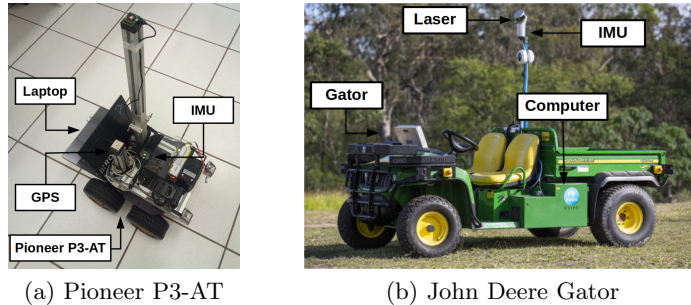


Fig. 3: Mobile robotic platforms used in the experiments.

Data acquisition was performed in two outdoor environments, with different levels of roughness and slope. The first outdoor environment contains five different Levels of Roughness (LR). The Levels of Roughness in first environment are: *i*) LR1 - Low level of roughness; *ii*) LR2 - Medium-low level of roughness; *iii*) LR3 - Medium level of roughness; *iv*) LR4 - Medium-high level of roughness; and *v*) LR5 - High level of roughness. The second outdoor environment contains different levels of roughness and slope, including regions such as a parking lot, building areas, and bush-land. The Pioneer P3-AT and Gator robots were used in first and second outdoor environments, respectively.

#### 3.2 Speed-Invariant Transformation Evaluation

This experiment evaluates the quality of the proposed Inertial Speed-Invariant Transformation (ISIT). Inertial measurements acquired at different speeds are transformed in corresponding inertial signals at a constant speed. In Fig. 4 are presented the raw and the transformed Linear Accelerations in Z-axis, for area 1. From Fig. 4 it is possible to visually observe that transformed inertial data, even at different speeds, present reduced inertial magnitude variations.

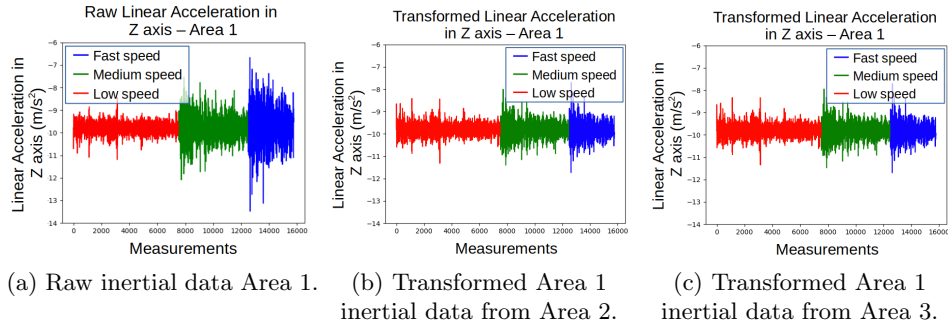


Fig. 4: Raw and speed-invariant inertial data, for different speeds. In Fig. 4a, the raw inertial data in area 1 can be seen. In Figs. 4b and 4c, the transformed inertial data is shown.

In Table 1 we observe the high magnitude dispersion, computed from raw inertial data, for different areas and speeds. Higher dispersion equates to higher inertial magnitude variation between different speeds. In Table 2, we observe the magnitude dispersion, computed from transformed inertial data, comparing different predictive models, areas, and speeds.

Table 1: Dispersion of raw inertial magnitudes, with different areas and speeds.

	Area 1	Area 2	Area 3
<b>Dispersion of Raw Inertial Magnitudes</b>	210.982	279.043	78.664

Table 2: Dispersion of transformed inertial magnitudes, with different areas and speeds.

	Test			
	Area 1	Area 2	Area 3	
<b>2nd Degree Polynomial</b>	<b>Area 1</b>	2.022	28.394	2.425
	<b>Train Area 2</b>	2.294	32.847	1.853
	<b>Area 3</b>	2.181	28.572	2.277
<b>3rd Degree Polynomial</b>	<b>Area 1</b>	2.024	28.909	2.232
	<b>Train Area 2</b>	2.338	34.345	2.897
	<b>Area 3</b>	2.540	30.748	2.432
<b>Random Forest</b>	<b>Area 1</b>	2.187	31.673	2.108
	<b>Train Area 2</b>	2.622	37.129	0.922
	<b>Area 3</b>	2.318	32.049	2.789

From Tables 1 and 2, it is possible to verify that the transformed inertial data for all predictive models presented lower dispersion of magnitudes than raw inertial data. In other words, after the speed-invariant transformation, the different inertial data became more similar, regarding the magnitude variation.



Table 2 shows that the proposed ISIT model (2nd Degree Polynomial Regression) presents lower dispersion measurements in seven of nine scenarios.

### 3.3 Roughness Level Classification Evaluation

This experiment evaluates the accuracy of the proposed roughness level classification process. In this assessment, for the same environment and the same speed, different sets of inertial data are used to train and test the classification models. Train and test inertial data were collected in different environments to avoid overfitting in the training process. Additionally, three different classification models are evaluated: *i*) Random Forest; *ii*) Ada Boosting; and *iii*) Support Vector Machine (SVM). These classification models are used due to good results obtained in the classification terrain context [10][3][8].

Table 3: Results for roughness level classification on outdoor terrains. In this experiment are presented the accuracy for Random Forest, regarding three different speeds, for each run.

		Speed	Test		
Random Forest	0.4		run 1	run 2	run 3
		Train	run 1	run 2	run 3
		run 1	run 2	run 3	
	0.6		run 1	run 2	run 3
		Train	run 1	run 2	run 3
		run 1	run 2	run 3	
	0.8		run 1	run 2	run 3
		Train	run 1	run 2	run 3
		run 1	run 2	run 3	

Table 3, shows roughness level classification results, only for the better classification model. Results show that the proposed Random Forest classification model presents high accuracy in tackled classification problems. Additionally, our proposed classification model achieves a mean accuracy of: *i*) 93.9% for 0.4 m/s, with a standard deviation of 0.020; *ii*) 95.4% for 0.6 m/s, with a standard deviation of 0.006; and *iii*) 84.1% for 0.8 m/s, with a standard deviation of 0.063. The results of the best baseline technique were achieved by SVM model, with mean accuracy of: *i*) 89.4% for 0.4 m/s; *ii*) 86.9% for 0.6 m/s; and *iii*) 79.6% for 0.8 m/s.

### 3.4 Outdoor terrain mapping evaluation

In this experiment, we evaluate the estimated outdoor terrain maps and the estimated navigation costs, to measure the accuracy of the proposed outdoor terrain mapping approach. In Fig. 5, are presented the baseline outdoor terrain map (using Random Forest regression) and the proposed outdoor terrain map

(using CNN predictive model). The baseline regression technique is used due to good results obtained in terrain analysis predictions [9]. From Fig. 5, it is possible to observe the adequate representation of flat regions, regions with smooth transitions (like slopes in terrain), and rugged regions.

Table 4 shows the obtained navigation costs. We observe that path costs computed from the proposed CNN approach are lower than path costs computed from the baseline approach.

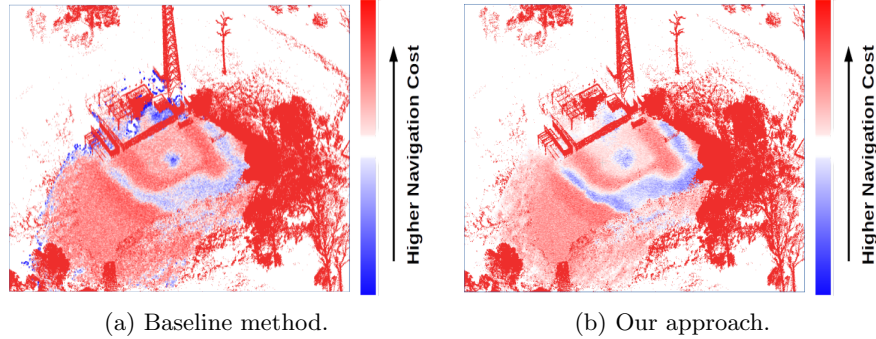


Fig. 5: Outdoor terrain maps for Environment 2 - Area 2.

Table 4: Path costs generated by motion planner accordingly to different predictive models on different terrains.

Path	Path costs			
	Baseline		Methodology	
	Area 4	Area 2	Area 4	Area 2
<b>1</b>	10.41	11.38	1.55	1.28
<b>2</b>	25.27	51.18	2.20	9.18
<b>3</b>	16.38	57.48	1.34	7.54
<b>4</b>	17.15	44.16	1.27	4.58
<b>5</b>	24.31	26.49	3.79	2.04

### 3.5 Outdoor terrain mapping effectiveness

This experiment focuses on evaluating the effectiveness of the proposed outdoor terrain mapping approach. In Fig. 6 are presented different trajectories, computed from the proposed outdoor terrain map, regarding *i*) only distance (green) and; *ii*) only navigation cost (orange). The path length considering only distance is 407.08 meters, while path length considering only navigation cost is 425.72 meters. The path cost considering only distance is 488.15, while the path cost considering only navigation cost is 5.81.

Table 5 presents the path costs computed from planned paths regarding distance and navigation cost. From Table 5, it is possible to verify the higher navigation costs for planned paths computed considering only the distance aspect. In this sense, regarding the obtained results, we can state that a 3D Augmented

Terrain Map with navigation costs increases the efficiency and safety navigation for ground robots in outdoor environments.

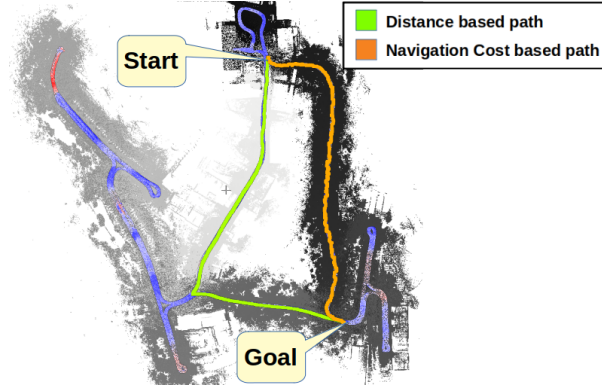


Fig. 6: Trajectories computed from outdoor terrain map: i) distance (green) and; ii) navigation cost (orange).

Table 5: Path costs computed from the proposed outdoor terrain mapping according to different metrics (distance or navigation cost) on different terrains.

Path costs			
	Terrain	Distance	Navigation Cost
<b>Paths</b>	4	488.15	5.81
	4	74.35	2.31
	2	91.91	8.42
	2	35.23	5.72
	2	51.85	4.20

## 4 Conclusion and Future Work

In this work, we addressed the problem of creating an outdoor terrain map based on inertial and laser sensors. Unlike other state-of-the-art approaches, our method considers inertial speed-invariant measurements, combined with laser measurements, to estimate the environment navigation costs providing a rich 3D terrain map.

This work’s major contribution is the proposition of an approach to predict navigation costs, from untraveled regions represented as point clouds, through Deep Learning. Moreover, creating a three-dimensional augmented terrain map provides efficient complementary information to decision-making in path planning tasks on outdoor environments.

Real-world experiments performed on environments with different terrains showed that the generated maps are reliable and accurate, considering the computed path costs. The proposed inertial speed-invariant transformation proved

to be an alternative to reduce the impact of speed change during robot motion in terrain analysis step. The accuracy obtained from the roughness level classification process showed a viable approach to represent and classify the roughness levels on outdoor terrains. Finally, we showed the use of CNN to estimate inertial navigation cost presented accurate results.

As future work, we intend to make the proposed outdoor terrain map representation more flexible to incorporate features from different types of sensors such as cameras. We also intend to study a strategy to make the inertial navigation cost invariant to the robot size.

## References

1. Bosse, M., Zlot, R.: Continuous 3d scan-matching with a spinning 2d laser. In: IEEE Int. Conf. on Robotics and Automation. pp. 4312–4319 (2009)
2. DuPont, E.M., Moore, C.A., Collins, E.G., Coyle, E.: Frequency response method for terrain classification in autonomous ground vehicles. *Autonomous Robots* **24**(4), 337–347 (May 2008)
3. Dutta, A., Dasgupta, P.: Ensemble learning with weak classifiers for fast and reliable unknown terrain classification using mobile robots. *IEEE Transactions on Systems, Man, and Cybernetics: Systems* **47**(11), 2933–2944 (2017)
4. Genesio, N., Abuhashim, T., Solari, F., Chessa, M., Natale, L.: Mobility map computations for autonomous navigation using an RGBD sensor. *CoRR* (2016)
5. Guerrero, J.A., Jaud, M., Lenain, R., Rouveure, R., Faure, P.: Towards lidar-radar based terrain mapping. In: IEEE Int. Workshop on Advanced Robotics and its Social Impacts (ARSO). pp. 1–6 (June 2015)
6. Nardi, L., Stachniss, C.: Actively Improving Robot Navigation On Different Terrains Using Gaussian Process Mixture Models. In: IEEE ICRA (03 2019)
7. Oliveira, F.G., Alves Neto, A., Borges, P., Campos, M.F.M., Macharet, D.G.: Augmented Vector Field Navigation Cost Mapping using Inertial Sensors. In: 19th Int. Conf. on Advanced Robotics (ICAR). pp. 388–393 (Dec 2019)
8. Oliveira, F.G., Santos, E.R.S., Alves Neto, A., Campos, M.F.M., Macharet, D.G.: Speed-invariant terrain roughness classification and control based on inertial sensors. In: 2017 Latin American Robotics Symposium (LARS) and 2017 Brazilian Symposium on Robotics (SBR). pp. 1–6 (Nov 2017)
9. Ono, M., Fuchs, T.J., Steffy, A., Maimone, M., Yen, J.: Risk-aware planetary rover operation: Autonomous terrain classification and path planning. In: IEEE Aerospace Conf. pp. 1–10 (March 2015)
10. Otte, S., Laible, S., Hanten, R., Zell, A.: Robust visual terrain classification with recurrent neural networks. *European Symposium on Artificial Neural Networks, Computational Intelligence and Machine Learning* (01 2015)
11. Pfrunder, A., Borges, P.V.K., Romero, A.R., Catt, G., Elfes, A.: Real-time autonomous ground vehicle navigation in heterogeneous environments using a 3d lidar. In: IEEE/RSJ Int. Conf. on Intelligent Robots and Systems (IROS) (2017)
12. Rao, K.R., Kim, D.N., Hwang, J.J.: *Fast Fourier Transform - Algorithms and Applications*. Springer Publishing Company, Incorporated, 1st edn. (2010)
13. Sebastian, B., Ren, H., Ben-Tzvi, P.: Neural network based heterogeneous sensor fusion for robot motion planning. In: 2019 IEEE/RSJ International Conference on Intelligent Robots and Systems (IROS). IEEE (Nov 2019)